Scaling of an optimal slip wall model for LES of nonequilibrium turbulent boundary layers

By M. P. Whitmore, S. T. Bose AND P. Moin

Previous efforts in slip wall modeling for large-eddy simulation (LES) demonstrated the effectiveness of determining the scaling behavior of an optimal slip length model for turbulent channels at a wide range of friction Reynolds numbers. The scaling behavior of ideal slip length models for flows with pressure gradients and nonequilibrium effects is comparatively less well understood. Simulations of five adverse pressure gradient cases are performed, first using wall-resolved LES (WRLES) to determine reference quantities, then using the optimal slip wall modeling approach (Whitmore *et al.* 2023). The scaling of the optimal slip lengths is then investigated with respect to quantities of interest for pressure gradient boundary layers.

1. Introduction

Slip wall models for large-eddy simulation (LES), introduced by Bose & Moin (2014), present an alternative approach to modeling the effects of the unresolved near-wall flow on the outer LES solution. As opposed to wall-stress models, which typically rely on the assumption of an attached thin boundary layer and an equilibrium stress or velocity distribution, the slip wall model imposes a Robin boundary condition that is formally derived from the application of a low-pass filter to the Navier–Stokes equations, making no assumptions about the underlying flow. Because the slip wall model does not make the same assumptions as traditional wall-stress models, it has the potential for higher-fidelity representation of complex flows with pressure gradients and nonequilibrium effects, where the assumptions of traditional wall-stress models are violated.

Slip wall models for wall-modeled large-eddy simulation (WMLES) relate the filtered velocity components at the wall to their wall-normal gradients by a length scale called the slip length and, therefore, require the prescription of a slip length model. Earlier studies demonstrated the possibility of dynamic slip wall models, which adjust the slip length according to the characteristics of the LES solution at two different filter scales (Bose & Moin 2014; Bae *et al.* 2019). While these dynamic models have a strong potential for predictive WMLES because they require no prior knowledge of the flow state, they encounter difficulties arising from sensitivities to test filtering operations as well as subgrid-scale models. An alternative approach to the development of slip length models involves leveraging physical information from a simple flow configuration in order to determine an appropriate model.

The physics-based approach to developing an optimal slip length model has been investigated by Pradhan & Duraisamy (2022) through the use of an optimal Galerkin projection of direct numerical simulation data from a turbulent channel onto a coarse-grained finite-element basis (although the form of the slip boundary condition used therein differs from that of the present work). Similarly, Whitmore *et al.* (2023) presented an optimal slip wall model approach that specifies an objective function based on the error in the

skin friction predicted by a WMLES relative to a reference data set, which then minimizes this objective function by adjusting the slip length through the use of *a posteriori* simulations. This approach was applied to the flow through a turbulent channel at various Reynolds numbers and grid resolutions, yielding a data set of optimal slip lengths in each case. The authors observed a collapse of the data when scaling in viscous inner units and found a parameterization of the data. This parameterization was subsequently used as a slip length model for the slip length in equilibrium wall-bounded turbulent flows. In conjunction with a nonequilibrium flow sensor, Whitmore *et al.* (2024a,b) developed a sensor-based slip length model that demonstrated good prediction of complex flows over aircraft geometries at various Reynolds numbers and angles of attack.

While the sensor-based slip wall model has been demonstrated to perform well in a number of complex external aerodynamics cases, the aspects of the model used to capture nonequilibrium flow were not developed rigorously (i.e., they were not based on any specific physical or mathematical assumptions). In order to have greater confidence in the generalizability of a slip wall model for nonequilibrium flow, this study applies the optimal slip wall model approach to a suite of adverse pressure gradient boundary layers to collect a data set expressing the behavior of an ideal slip length model in a nonequilibrium flow. The resulting optimal slip length data are then analyzed to determine their scaling with varying nonequilibrium effects.

Section 2 of this brief discusses the mathematical framework of the optimal slip length model as well as the setup of the adverse pressure gradient boundary layer simulations. Sections 3 and 4 present the results of the WRLES and the optimal slip WMLES for the adverse pressure gradient boundary layer cases, respectively. Conclusions are offered in Section 5.

2. Mathematical framework

Following Bose & Moin (2014), the slip wall boundary condition for the LES filtered velocity field, $\overline{u}_i$, is written as

$$\overline{u}_i|_w = (C_{slip}\Delta_w)\left.\frac{\partial \overline{u}_i}{\partial n}\right|_w, \qquad \forall i \in \{1,2,3\}, \tag{2.1}$$

where Δ_w is the distance of the first off-wall grid cell center to the wall, n is the wall-normal coordinate, and C_{slip} is the nondimensional slip length coefficient. In general, the slip length may be a function of space. Here, the slip length is assumed to vary in one dimension as a function of the streamwise coordinate.

All of the simulations in this brief are performed using the code charLES (distributed by Cadence Design Systems), which is a second-order finite-volume solver for the compressible Navier–Stokes equations based on polyhedral meshes formed by centroidal Voronoi tessellations with GPU acceleration (Brès *et al.* 2022). The code is used for both WRLES and WMLES. The subgrid-scale model used in this study is the dynamic Smagorinsky model (Germano *et al.* 1991).

2.1. *Optimization problem*

We desire an objective function that is minimized when error in the skin-friction coefficient, $C_f = 2\tau_w/\rho U_\infty^2$, of the WMLES is minimized with respect to reference data. The

objective function J is defined according to Whitmore *et al.* (2023) such that

$$J\left(C_{slip}^{(k)}\right) = \frac{1}{2}\sum_{k}\left[\frac{1}{A_k}\int_{x\in\partial\Omega} w_k(x)\left\{C_f\left(x; C_{slip}^{(k)}\right) - C_f^{ref}(x)\right\}dx\right]^2 A_k, \tag{2.2}$$

where k is the index of the boundary element that is used to discretize the slip length in space over the boundary surface, w_k is the weight function of the element, and A_k is the weighted area of the element. The reference skin-friction coefficient C_f^{ref} is assumed to be known as a function of space and typically comes from some higher-fidelity data source, like an experiment, reference simulation, or analytical solution. Therefore, we seek the values of $C_{slip}^{(k)}$ that minimize the objective function. This optimization problem is solved by performing coordinate descent on the discretized slip length coefficient in space, where gradients are evaluated as finite differences from *a posteriori* WMLES calculations. The optimization steps are performed concurrently with the WMLES solution.

2.2. *Adverse pressure gradient boundary layers*

The adverse pressure gradient cases of interest follow those of Bobke *et al.* (2017), in which the freestream velocity U_∞ follows a power law

$$U_\infty \propto (x - x_0)^m, \tag{2.3}$$

where x_0 is the virtual origin and m is a constant exponent. The strength of the pressure gradient cases can be measured by the nondimensional Clauser parameter β, defined as

$$\beta \equiv \frac{\delta^*}{\tau_w}\frac{\partial P_e}{\partial x} = -\frac{\delta^*}{\tau_w}U_e\frac{\partial U_e}{\partial x}. \tag{2.4}$$

Five cases from Bobke *et al.* (2017) are investigated: two approximately constant Clauser parameter cases, $\beta \approx 1$ and $\beta \approx 2$, and three constant exponent cases, $m = -0.13, -0.16$, and -0.18. These cases exhibit a range of adverse pressure gradient strengths.

3. Wall-resolved LES of adverse pressure gradient boundary layers

Reference skin-friction coefficient profiles are required in order to perform the optimal slip WMLES of the adverse pressure gradient boundary layer cases. To obtain these reference skin-friction coefficient profiles, WRLES of the adverse pressure gradient boundary layers are performed using charLES. While it is possible to use the skin-friction coefficient data of Bobke *et al.* (2017) directly to solve for the optimal slip lengths, the use of this approach quickly encounters the challenge of matching domain setups between the present simulations and those of the reference data. The simulations performed by Bobke *et al.* (2017) used a fully spectral code for the incompressible Navier–Stokes equations, including full simulation of the transition to turbulence from a laminar Blasius boundary layer state. In comparison, the present simulations use a code that solves the compressible Navier–Stokes equations, leading to differences in the ways that boundary conditions are enforced. Additionally, for a WMLES it is not practical to simulate the entire transition-to-turbulence process from a laminar state. Instead, a recycling and rescaling boundary condition is employed at $x/\delta_0 = 200$ to shorten the domain and start the boundary layer simulation in a turbulent state (Whitmore *et al.* 2022). Because of the inevitable uncertainties arising from the differences in setup between the present WMLES and the simulations by Bobke *et al.* (2017), we elect to perform a suite of WRLES for the five adverse pressure gradient cases using the domain setup that the WMLES will use. These

Case	L_y	L_z	max $\frac{\Delta}{\delta_0}$	min $\frac{\Delta_s}{\delta_0}$	min $\frac{\Delta_n}{\delta_0}$	N_{CV} (Mcv)
$\beta \approx 1$	140	140	2	0.5	0.054	90
$\beta \approx 2$	180	180	2	0.5	0.054	121
$m = -0.13$	120	120	2	0.5	0.054	79
$m = -0.16$	180	180	2	0.5	0.054	121
$m = -0.18$	250	250	2	0.5	0.054	175

TABLE 1. Details of the WRLES meshes for the adverse pressure gradient cases.

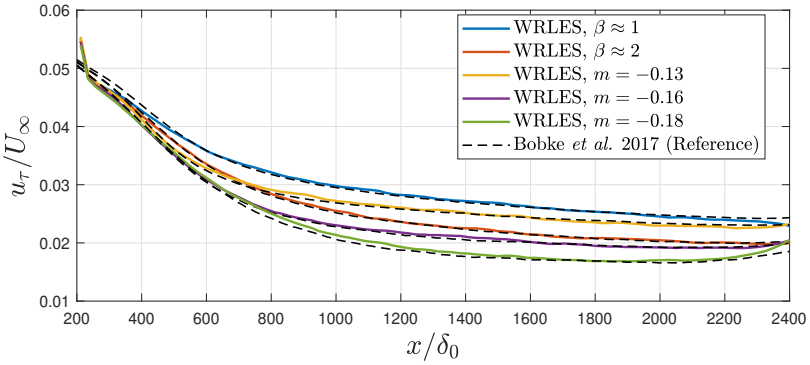

FIGURE 1. Friction velocity as a function of streamwise coordinate for the five adverse pressure gradient WRLES compared with the reference simulation.

WRLES are employed to obtain the reference data for the WMLES, which reduces the uncertainties related to differences in numerics and domain setup. Table 1 presents the details of the meshes used for the WRLES of the five adverse pressure gradient boundary layer cases. The freestream pressure gradients in these simulations are imposed through characteristic boundary conditions that prescribe the desired freestream velocity profiles. The domains are periodic in the spanwise direction. The domain outflow includes a free slip extension from $x/\delta_0 = 2500$ to 2700 where a Navier–Stokes characteristic boundary condition is imposed to enforce a constant mass flux.

Figure 1 plots the average friction velocity as a function of the streamwise coordinate. The figure shows that stronger adverse pressure gradients, corresponding to higher β and more negative m values, lead to a larger drop in the friction velocity in the downstream portion of the domain. The results of the present WRLES cases also agree qualitatively well with the friction velocity found by Bobke *et al.* (2017). One area where the present WRLES disagree with the reference is upstream, near $x/\delta_0 = 200$. The dip in the present results is caused by a short development region behind the recycling and rescaling inlet boundary condition. The data here are not expected to match those of Bobke *et al.* (2017) because the upstream transitional boundary layer is not resolved. Additionally, there is a discrepancy near the flow outlet, which is caused by the use of a Navier–Stokes characteristic boundary condition for the outflow compared with the fringe method used by Bobke *et al.* (2017).

Figure 2 plots the first grid cell half-height in inner units, y_1^+. The values range from approximately 0.65 in the upstream portion of the domain to 0.2 further downstream,

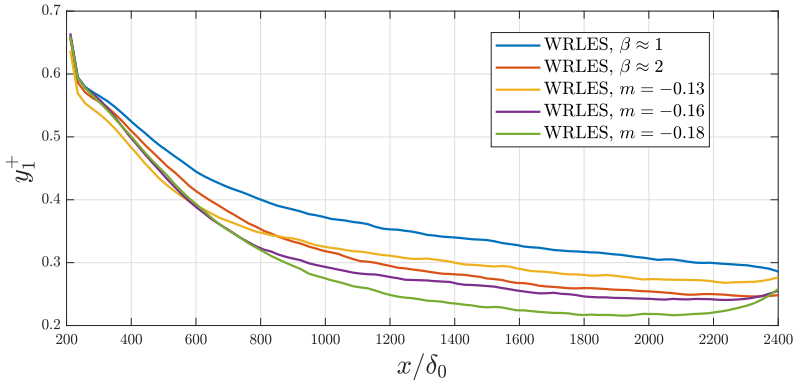

FIGURE 2. First cell wall-normal resolution in inner units as a function of the streamwise coordinate for the five adverse pressure gradient WRLES.

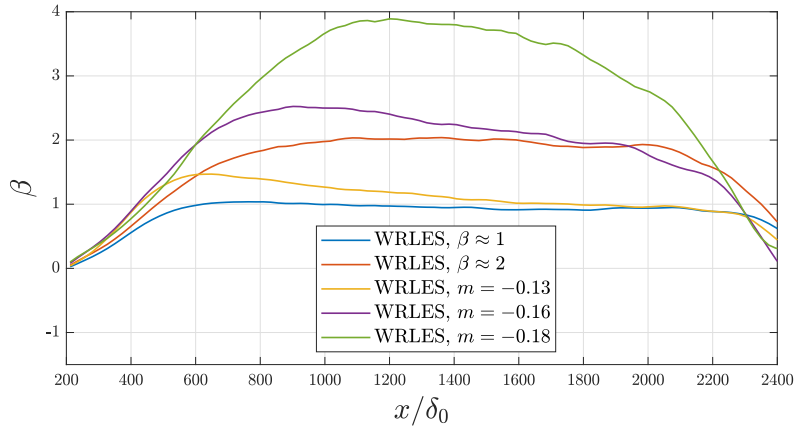

FIGURE 3. Clauser parameter of the five adverse pressure gradient boundary layer WRLES.

suggesting that the grid resolution is adequate in the wall-normal direction to capture the sharp velocity gradients arising from the no-slip boundary condition. Figure 3 plots the Clauser parameters from these five WRLES cases. The Clauser parameter profiles for the $\beta \approx 1$ and $\beta \approx 2$ cases are shown to be relatively flat for most of the domain at the expected values. The values for the constant m cases show an increasingly positive Clauser parameter for the larger negative m values, indicating a stronger adverse pressure gradient.

4. Optimal slip wall-modeled LES of adverse pressure gradient boundary layers

The five adverse pressure gradient boundary layer cases are now simulated using WMLES while applying the optimal slip length approach. The domain setup of the cases is the same as in the WRLES cases. In order to distribute the grid points in a cost-effective manner while also avoiding excessive grid refinement of the boundary layer in the downstream region of the domain, the meshes for the WMLES are designed to be boundary layer conforming, such that the number of grid cells that fit inside the local

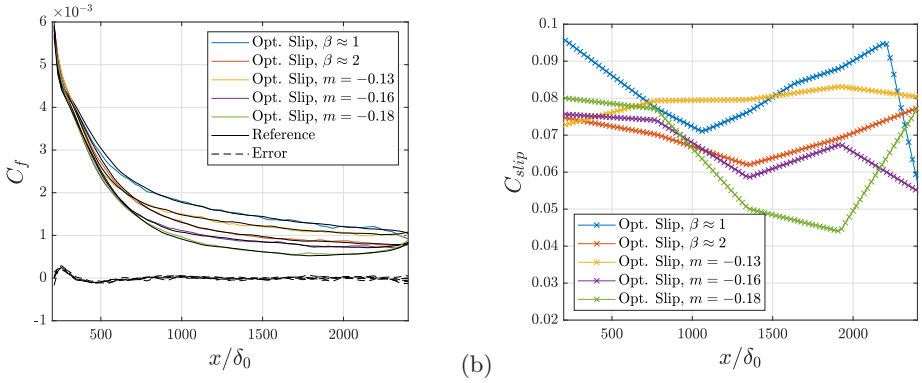

FIGURE 4. (a) Skin-friction coefficients from the five optimal slip WMLES cases compared with the reference skin-friction coefficient profiles. The local error in the skin-friction coefficient is also plotted and shows qualitative convergence. (b) Optimal slip length coefficients as a function of the streamwise coordinate.

boundary layer thickness is held constant. The isotropic grid length scale, Δ, varies as a function of the streamwise coordinate such that $\delta_{99}(x)/\Delta(x) \approx 8$ for the WMLES presented. Figure 4(a) plots the resulting skin-friction profiles from the WMLES for the five cases and compares them with the reference skin-friction coefficient values, along with a plot of the local error in the skin-friction coefficient from the five cases. The cases have converged qualitatively well. Figure 4(b) shows the profiles of the slip length coefficient as a function of the streamwise coordinate. Most of the cases use five uniform discrete control points to represent the slip length coefficient as a function of space, while the $\beta \approx 1$ case uses nine uniform control points. While more control points could be used to improve the local accuracy of the skin-friction coefficient profiles of the WMLES, doing so would also result in a more difficult optimization problem. Future work could look into improved representations of the slip length coefficient profiles in space, through either more control points or more judicious placement of those control points.

To investigate the scaling behavior of the optimal slip length data, we hypothesize that the slip length coefficient can be expressed as a function

$$C_{slip}(y_1^+, q) = C_{slip}^{eq}(y_1^+) f(q), \tag{4.1}$$

where $C_{slip}^{eq}(y_1^+)$ denotes the parameterization of the equilibrium optimal slip length coefficients, as previously identified in the turbulent channel (Whitmore *et al.* 2023), and $f(q)$ denotes some function of q, which is an as-yet-undetermined parameter to quantify nonequilibrium effects. This hypothesis is restrictive in that it assumes the modulation of the slip length coefficient with nonequilibrium effects can be represented by a multiplicative factor and can also be represented as a function of only one nonequilibrium flow parameter. The use of a multiplicative factor is justified because it naturally retains the proper convergence to the no-slip condition in the limit of fine grid resolution. The choice of a single parameter to quantify nonequilibrium effects is practical because of the limited data in the present work and could be relaxed in the future given more data for flows with different pressure gradients or a better understanding of the physical scalings that govern nonequilibrium flows.

To test this hypothesis, we first investigate whether the equilibrium parameterization of the optimal slip length coefficients from the turbulent channel can capture the present data. Figure 5 plots the optimal slip length coefficients as a function of y_1^+. It is clear that

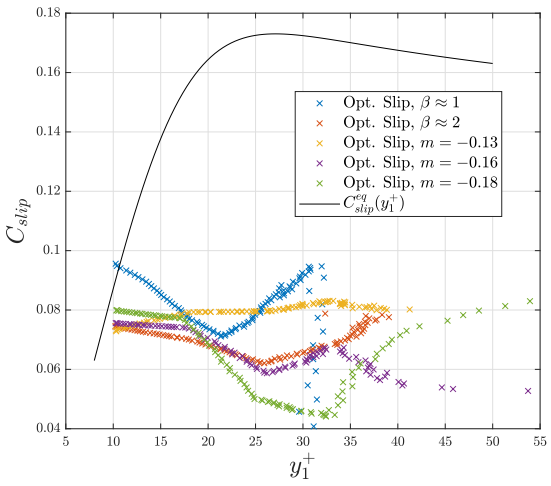

FIGURE 5. Optimal slip length coefficient data from the adverse pressure gradient boundary layers, plotted as a function of the local wall-normal grid resolution in inner units, y_1^+. These data are compared with the equilibrium parameterization from the turbulent channel data obtained by Whitmore *et al.* (2023).

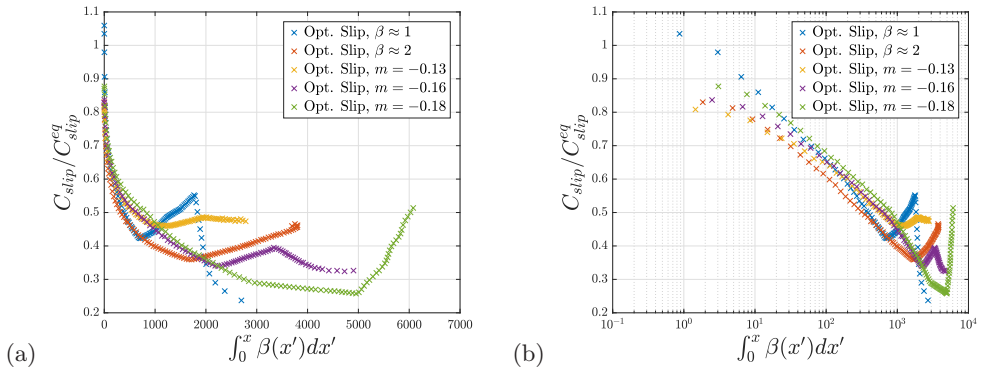

FIGURE 6. (a) Optimal slip length coefficients from the adverse pressure gradient boundary layer cases, normalized by the equilibrium parameterization, plotted against a nonequilibrium flow parameter. In this case, the chosen nonequilibrium flow parameter is a cumulative Clauser parameter, integrated in the streamwise direction. (b) The same plot in semilog coordinates demonstrates consistent early decay behavior across different pressure gradient cases.

the present data from the adverse pressure gradient boundary layers is not well captured by the parameterization from Whitmore *et al.* (2023). Upstream, where the boundary layer is in a zero pressure gradient state, the slip length coefficients agree with the equilibrium parameterization; however, moving downstream as the adverse pressure gradient effects accumulate, the data move further away from the equilibrium parameterization. This behavior of moving away from the equilibrium slip length scaling is what we seek to characterize in terms of a nonequilibrium flow parameter.

As a first attempt to characterize the behavior of the optimal slip length coefficients with pressure gradient effects, Figure 6 plots the slip length coefficient data, normalized

by the local equilibrium slip length, as a function of a cumulative Clauser parameter,

$$q \equiv \int_0^x \beta(x')dx', \tag{4.2}$$

which is integrated along the streamwise coordinate beginning in the zero pressure gradient region. Notably, the slip length coefficient data show some initial collapse for the lower cumulative β values. Figure 6(b) shows this initial collapse in semilog coordinates, where the five cases appear to exhibit an approximately exponential decay of the ideal slip length coefficients from their equilibrium value in the upstream zero pressure gradient region. Ultimately, this collapse does not continue through the entire domain, suggesting that the choice of the cumulative β parameter does not fully capture the influence of the pressure gradient effects on the optimal slip length coefficients. The figure shows that all five pressure gradient cases begin to trend upward at some value of cumulative β, which is different for each case. This upward trend appears at higher values of cumulative β for the cases with increasing adverse pressure gradient strength. It is important to note that the cumulative Clauser parameter includes an implicit length scale that is presently not normalized by a physically relevant length scale. It is possible that the appropriate length scale to normalize this quantity is associated with the upstream distance over which the pressure gradient history is still influencing the local flow. Agrawal *et al.* (2024) showed that the local flow becomes insensitive to its pressure gradient history after evolving over some streamwise length but that this length can vary significantly between different pressure gradient cases. The normalization by such a length scale that captures the relevant pressure gradient history may help to address the downstream behavior where the data from the five cases begin to diverge at different points.

While this attempt at parameterization of the data with cumulative β is not sufficient for modeling purposes, the similar qualitative trends for all five adverse pressure gradient cases suggest that a data collapse may be found either by using a different nonequilibrium flow parameter, by identifying an appropriate length scale normalization for the pressure gradient history, or by introducing a secondary parameterization that can account for the behavior at a later region in the domain. Ultimately, further investigation and more data are needed to adequately characterize the behavior of these optimal slip length coefficients with nonequilibrium effects such that they can be used to inform a slip length model.

5. Conclusions

Physics-based modeling of slip length coefficients can effectively capture complex flows including applications in external aerodynamics. Previous models used a parameterization for slip length coefficients informed by an optimal slip length model approach applied to turbulent channels (Whitmore *et al.* 2023); however, these models did not incorporate any information about the scaling of optimal slip length coefficients with nonequilibrium effects. To inform more robust slip wall models for capturing nonequilibrium flows, we applied the optimal slip length model approach to a suite of five adverse pressure gradient boundary layers to investigate the optimal slip length scaling behavior.

In order to obtain high-quality reference data that are also obtainable with coarser WMLES calculations, the WRLES of the five adverse pressure gradient cases was performed following the simulations by Bobke *et al.* (2017). The WRLES calculations show overall qualitative agreement with those of Bobke *et al.* (2017) but also demonstrate discrepancies arising from differences in the domain setup, such as the use of a recycling and rescaling inflow boundary condition. The present WRLES skin-friction coefficient

data are used as a high-quality reference data set, which employs a domain setup that exactly matches the one used in the WMLES calculations. As a result, the optimal slip length approach can be used more effectively than if the skin-friction data from Bobke *et al.* (2017) were used directly as reference data.

The optimal slip length model approach was applied to the five adverse pressure gradient boundary layer cases for one WMLES grid resolution, specifically the case of a boundary layer conforming mesh with a constant eight grid cells inside the boundary layer thickness over the length of the domain. The WMLES using the optimal slip length approach exhibited good convergence with the skin-friction coefficient data. The resulting optimal slip length data were analyzed to determine whether the nonequilibrium effects could be characterized. An initial attempt showed some collapse of the optimal slip length data using a cumulative Clauser parameter, integrated in the streamwise direction. Specifically, an initial exponential decay of the slip length coefficient was observed across cases with increasing cumulative Clauser parameter. While a modest collapse of the data was observed in the upstream half of the domain where the pressure gradient effects begin, further downstream in the domain, the data began to diverge. More work is needed both to collect more optimal slip length data and to better characterize the effect of pressure gradients on the optimal slip length values.

Acknowledgments

This research is supported by the NASA Transformation Tools and Technologies project (grant 80NSSC20M0201). This research used resources of the Oak Ridge Leadership Computing Facility at the Oak Ridge National Laboratory, which is supported by the Office of Science of the U.S. Department of Energy under Contract No. DE-AC05-00OR22725.

REFERENCES

Agrawal, R., Bose, S. T., Griffin, K. P. & Moin, P. 2024 An extension of Thwaites' method for turbulent boundary layers. *Flow* **4**, E25.

Bae, H. J., Lozano-Durán, A., Bose, S. T. & Moin, P. 2019 Dynamic slip wall model for large-eddy simulation. *J. Fluid Mech.* **859**, 400–432.

Bobke, A., Vinuesa, R., Örlü, R. & Schlatter, P. 2017 History effects and near equilibrium in adverse-pressure-gradient turbulent boundary layers. *J. Fluid Mech.* **820**, 667–692.

Bose, S. T. & Moin, P. 2014 A dynamic slip boundary condition for wall-modeled large-eddy simulation. *Phys. Fluids* **26**, 015104.

Brès, G. A., Bose, S. T., Ivey, C. B., Emory, M. & Ham, F. 2022 GPU-accelerated large-eddy simulations of supersonic jets from twin rectangular nozzle. *AIAA Paper 2022-3001.*

Germano, M., Piomelli, U., Moin, P. & Cabot, W. H. 1991 A dynamic subgrid-scale eddy viscosity model. *Phys. Fluids* **3**, 1760–1765.

Pradhan, A. & Duraisamy, K. 2022 A unified understanding of scale-resolving simulations and near-wall modelling of turbulent flows using optimal finite-element projections. *J. Fluid Mech.* **955**, A6.

Whitmore, M. P., Bose, S. T. & Moin, P. 2022 Progress on slip wall modeled LES for predicting smooth body separation. *Annual Research Briefs*, Center for Turbulence Research, Stanford University, pp. 59–70.

Whitmore, M. P., Bose, S. T. & Moin, P. 2023 Evaluation of an optimal slip wall

model for large-eddy simulation. *Annual Research Briefs*, Center for Turbulence Research, Stanford University, pp. 283–294.

Whitmore, M. P., Bose, S. T. & Moin, P. 2024a Slip-wall-modeled large-eddy simulation for prediction of turbulent smooth-body separation. *AIAA Paper 2024-2374*.

Whitmore, M. P., Bose, S. T. & Moin, P. 2024b Application of a sensor-based slip wall model in the presence of pressure gradient effects. *Annual Research Briefs*, Center for Turbulence Research, Stanford University, pp. 219–229.